Journal of Atmospheric and Solar-Terrestrial Physics 163 (2017) 46–53

Contents lists available at ScienceDirect

Journal of Atmospheric and Solar-Terrestrial Physics

journal homepage: www.elsevier.com/locate/jastp

# Long term variabilities and tendencies of mesospheric lunar semidiurnal tide over Tirunelveli (8.7°N, 77.8°E)

S. Sathishkumar [a,*], S. Sridharan [b], P.V. Muhammed Kutty [a], S. Gurubaran [c]

[a] Equatorial Geophysical Research Laboratory, Krishnapuram, Tirunelveli, 627011, India
[b] National Atmospheric Research Laboratory, Gadanki, Tirupati, 510112, India
[c] Indian Institute of Geomagnetism, New Panvel, Navi Mumbai, 410218, India

ARTICLE INFO

*Keywords:*
Lunar tide
Middle atmospheric dynamics
Climatology and planetary waves

ABSTRACT

The medium frequency radar deployed at Tirunelveli (8.7°N, 77.8°E), which is located near the southmost tip of peninsular India, have been providing continuous data from the year 1993 to the year 2012 that helped to study the long term tendencies in the lunar tidal variabilities over this geographic location. In the present paper we present the results of seasonal, interannual and long-term variabilities of lunar semi-diurnal tides in the upper mesosphere over Tirunelveli. The present study also includes comparison with model values. The study shows that the tidal amplitudes are larger in the meridional components of the mesospheric winds than the zonal winds. The seasonal variations of the tides are similar in both the components. The tides show maximum amplitudes of about ~5 m/s in February/March, secondary maximum amplitudes of about ~3 m/s in September and minimum amplitudes during summer months (May–August). The observed seasonal variation of the lunar tides do not compare well with Vial and Forbes (1994) model values, though it is consistent with earlier observations. The lunar tidal phase in meridional winds leads that in zonal winds from January to June and from September to November, while the latter leads the former during July/August. The lunar tides show large interannual variability. There are unusual amplitude enhancements in the lunar tide in meridional winds during the winters of 2006 and 2009, when major sudden stratospheric warmings (SSW) occurred at high latitude northern hemisphere, whereas zonal lunar tide does not show any clear association with the SSW. Vertical wavelengths of lunar tides in zonal and meridional wind are in the range of 20–90 km. The vertical wavelengths of lunar tides in both zonal and meridional component are smaller in June and larger in November and December. The monthly mean zonal and meridional winds are subjected to regression analysis to study the tidal response to long-period oscillations, namely, quasi-biennial oscillation (QBO), solar cycle variation and El-nino southern oscillation (ENSO). It is found the lunar tide in both zonal and meridional winds show significant QBO response, whereas zonal tide only shows significant negative response to solar cycle and positive response to ENSO. Besides, zonal tide only shows significant long-term increasing trend.

## 1. Introduction

The energetic in the mesosphere and lower thermosphere (MLT region) have direct influence on the dynamics and electrodynamics in the ionosphere. Variabilities in the energetic give rise to modifications in E region dynamo and thereby show up in the ionospheric currents. The variabilities in the energetic of MLT region is mainly produced by the tides and waves generated in, propagated through and broken in the MLT region. Atmospheric tides can be generated either by the absorption of solar radiation by different chemical species in different regions of the atmosphere or by the lunar gravitational excitation (Chapman and Lindzen, 1970). The absorption of solar radiation by water vapor in troposphere, ozone in the stratosphere and nitrogen and oxygen in the mesosphere excites various tidal modes in the respective regions. Solar tides have been studied extensively both theoretically and observationally and their contribution to the energetics of mesosphere and lower thermosphere (MLT) and variabilities of ionosphere, in particular over low-latitudes are well recognized (Forbes and Groves, 1987; Burrage et al., 1995; Pancheva et al., 2002). Lunar tides in the atmosphere which are predominantly semi-diurnal with period of 12.42 h are relatively less

* Corresponding author.
*E-mail addresses:* sathishmaths@gmail.com (S. Sathishkumar), sridhar.aiyer@gmail.com (S. Sridharan), mk.egrl.iig@gmail.com (P.V. Muhammed Kutty), su.gurubaran@gmail.com (S. Gurubaran).

http://dx.doi.org/10.1016/j.jastp.2017.05.015
Received 27 January 2017; Received in revised form 25 May 2017; Accepted 26 May 2017
Available online 29 May 2017
1364-6826/

studied because of their small amplitudes and its proximity in frequency to the solar semidiurnal tide makes the extraction of lunar tidal characteristics without spectral leakage from solar tides difficult. The lunar tides in the atmosphere are generated in the lower atmosphere primarily as result of the Moon's gravitational attraction and also due to vertical motion of Earth and ocean at the lower boundaries. The behaviors of the atmospheric medium through which lunar tides propagate have direct impact on the nature of the lunar tides. They sometimes get modified, suppressed or enhanced depending on the background conditions. Even though lunar tides exhibit a variety of different modes, the most pronounced mode visible in the day-to-day variability is the lunar semidiurnal tide (12.42 h) tide. In recent years, the lunar tide has attracted greater attention as an important element of ionosphere and thermosphere variability particularly over low-latitudes (Fejer et al., 2010; Park et al., 2012; Pedatella et al., 2012; Sathishkumar and Sridharan, 2013 to state a few).

Observations of lunar tides in the MLT have been made using various ground based instruments. Medium frequency (MF) radars (e.g. Stening and Vincent, 1989; Schlapp and Harris, 1993; Stening et al., 1995, 1997), meteor radars (e.g. Tsuda et al., 1981, Niu et al., 2005; Sanford et al., 2006, 2007) and LF-D1 technique (Stening and Jacobi, 2001) are a few to say. The above studies in the past have revealed that the horizontal winds associated with the lunar tide can reach amplitude as large as ~10 m/s in the MLT region. Stening et al. (1997, 2003) observed that the equatorial lunar tides in MF/meteor radar mesospheric winds over Christmas Island (2°N, 157°W) and Jakarta (6°S, 256°W) showed maximum amplitudes around mid winter and autumn in Northern Hemisphere. Vertical wavelengths were observed to be quite short, ranging from ~17 km to ~80 km. Stening et al. (1994) investigated the large scale latitudinal structure of the lunar semidiurnal tide, and found that it is latitudinally symmetric during solstice and asymmetric around equinox. Despite excellent beginning in the studies of lunar tide in the MLT region in the past, considerable progress has not been made because of paucity of long period observations that are necessary to reliably extract the lunar semidiurnal tide.

Using several years of observations of lunar semidiurnal tides using meteor radar observations from Wuhan, China by Niu et al. (2007) reported seasonal and interannual variabilities of lunar semi-diurnal tides at various altitudes. Their finding revealed that the phases of lunar tide did not agree with the values obtained from the GSWM model. Such contradiction necessitates more studies into the problem of lunar tidal variability using both ground and space borne observations. There were several attempts to study the tidal variabilities in the upper atmosphere even though much of them focused mainly on solar tides. Recently, Truskowski et al. (2014) analyzed the possible origins of the most prominent tides in the lower thermosphere and the nature of their seasonal and latitudinal structures using Sounding of the Atmosphere Broadband Emission Radiometry (TIMED/SABER) temperature measurements. They found considerable nonlinear interactions leading to generation of many spectral components. Another report by Laskar et al. (2014) that focused on the low latitude upper atmosphere used two independently measured upper atmospheric parameters namely, EEJ and TEC, to study the vertical coupling during Sudden Stratospheric warming (SSW) event and their dependence on solar activity. It seems there is a shortage of detailed studies on lunar semidiurnal tides in the upper atmosphere which are very crucial in the atmospheric electrodynamics. Pedatella and Forbes (2010) found that the lunar semidiurnal tide shows significant hemispheric asymmetry in the total electron content from November to February.

Only a few attempts were made in the past to model lunar tides and the one proposed by Vial and Forbes (1994) used a comprehensive forcing in the model and gives the latitudinal variations. Vial and Forbes (1994) model is a zonal mean model which considered the seasonal variability of the lunar tide from the ground to a height of 105 km. In this model, the lunar tidal amplitudes were predicted to reach up to ~10 m/s n the upper mesospheric heights. The model shows maximum during solstice and minimum during equinox over equator. The effects of background wind and temperature on the vertical propagation of lunar semi-diurnal tides into the MLT region were considered in the model of Stening et al. (1997). They also suggested that the interannual variability of lunar tides over Saskatoon, Canada may be explained by introducing stratospheric warming into the model. Recent works have shown a significantly enhanced effect of lunar semidiurnal tide in the equatorial electrojet and vertical drift velocity during the times of high-latitude sudden stratospheric warming (SSW) events (Fejer et al., 2010; Park et al., 2012). Pedatella et al. (2012) using model simulation showed that enhanced lunar tides during SSWs are of significant importance of generating the low latitude ionosphere perturbation during these periods. Also, Pedatella et al. (2014) studied tidal variability during 2009 sudden stratospheric warming (SSW) event using different model simulation. They found that evolution of the amplitude and phase of the migrating semidiurnal tide over time are similar even though their absolute values are different.

Luhr et al. (2012) used magnetic field measurements by the CHAMP (Challenging Minisatellite Payload) to study the global trends in lunar tide. Forbes et al. (2013) derived lunar tides using TIMED/SABER data and compared the values with the GSWM (global scale wave model) values. However, more studies on variabilities of lunar semi-diurnal tide with long-term data sets are necessary to better understand the coupling of neutral dynamics and ionospheric electrodynamics, as the lunar tide has been realized as a vital player in variabilities of the electrodynamics of the low-latitude ionosphere.

The present study reports the lunar semidiurnal tidal variabilities in the upper mesospheric region over a low latitude station, Tirunelveli which is located at the southern tip of the Indian peninsula. The observational data of this radar from January 1993 to December 2012 provide us an opportunity to study the seasonal, interannual and long-term variabilities and tendencies of lunar semidiurnal tide in the equatorial latitude and the results are compared with the Vial and Forbes (1994) model values.

## 2. Data analysis

The MF radar established at Tirunelveli (8.7°N, 77.8°E) has been providing nearly continuous wind observations in the altitude region 80–98 km with good data acceptance rate. The operational frequency is 1.98 MHz which gives partial reflections from the mesosphere – lower thermosphere (MLT) region above the station. Diurnal (24 h), semidiurnal (12 h), and terdiurnal (8 h) are the most dominant solar tidal modes. Among lunar tides, the migrating lunar semidiurnal tide of periods 12.416–12.424 h shows large amplitudes. Since the frequencies of the lunar and solar tides are very close, extended data sets are thus required to provide the spectral resolution necessary to resolve the lunar and solar components. Monthly window of hourly winds at each height is assumed to consist of a mean wind, sinusoidal planetary wave components, solar (diurnal, semidiurnal, and terdiurnal components) and lunar tidal (semidiurnal component) oscillations, as can be seen from the following equation:

$$U = U_0 + \sum_{n=1}^{l}\left[A_n cos\left(\frac{2\pi n}{L}t\right) + B_n sin\left(\frac{2\pi n}{L}t\right)\right] + \sum_{n=1}^{3}\left[C_n cos\left(\frac{2\pi n}{24}t\right) + D_n sin\left(\frac{2\pi n}{24}t\right)\right] + A_L cos\left(\frac{2\pi}{12.42}\tau\right) + B_L sin\left(\frac{2\pi}{12.42}\tau\right) \quad (1)$$

where $U_0$ is mean wind, L is the total data length (here 30 days of hourly data), n is the number of harmonics required to include all long-period planetary waves periods (here $l = 15$ so that waves with periods from 30 to 2 d are included in the fit. Here t is the solar time and $\nu$ is the lunar age giving a measure of the phase of the Moon from new Moon, i.e at the new moon, the lunar age is equal to zero and full moon is one. The tidal amplitudes and phases are computed using least squares method (Stening et al., 1994; Paulino et al., 2012; Sathishkumar and Sridharan, 2013).

As this method of computation gives reasonable amplitudes for lunar tides and the lunar tidal phases computed shows shift toward later hours on each months, which is a typical behavior of lunar tides, this method is used in the present study. Then the data window is shifted by each month successively to compute monthly variation of lunar tidal amplitude and phases. In the present work, seasonal and interannual variabilities of lunar semidiurnal tide are examined and the results are compared with Vial and Forbes (1994) model values. As the lunar tidal variations in zonal and meridional winds are expected to contain natural periodic signals, like the quasi-biennial oscillation (QBO), El-Nino Southern Oscillation (ENSO) and solar cycle (SC), a regression model is used to extract each signal quantitatively (Randel and Cobb, 1994; Sridharan et al., 2010). The general expression for the regression model equation at each altitude is given by

$$U(t) = \alpha(t) + \beta(t)\cdot t + \gamma(t)\cdot QBO(t) + \delta(t)\cdot solar(t) + \varepsilon(t)\cdot Enso(t) + resid(t). \tag{2}$$

where α(t) in the above equation have the form $\alpha(t) = A_0 + \sum_{i=2}^{12}[A_i \times Cos\omega_i t + B_i \times Sin\omega_i t]$, where $\omega_i = \frac{2\pi i}{24}$.

The lunar semi-diurnal tidal amplitudes s in zonal and meridional winds are subjected to this linear regression model and the coefficients α, β, γ, δ, and ε are determined in least square sense. α(t) represents seasonal and intraseasonal variations. If 'S' is the sum of square of residuals, 'n' is data length and 'p+1' is the number of coefficients to be determined, then the error in the estimation of coefficients are given by

$$\sigma = \sqrt{\frac{S}{n-p-1}(X^T X)^{-1}} \tag{3}$$

where X is the matrix of the regressors (Sridharan et al., 2010).

We have used Singapore monthly-mean QBO zonal winds (m/s) at 30 hPa as a QBO proxy, F10.7 solar radio flux as solar proxy, and Southern Oscillation Index (SOI), which is the normalized Tahiti (18°S, 150°W) minus Darwin (13°S, 131°E) monthly-mean sea-level pressures (hPa), as ENSO proxy, corresponding to the months t. The QBO winds for 70-10 hPa and SOI data were downloaded from the website http://www.geo.fu-berlin.de/met/ag/strat/produkte/qbo and http://www.cpc.ncep.noaa.gov/data/indices/soi respectively The solar flux data were obtained from ftp://ftp.geolab.nrcan.gc.ca/data/solar_flux/monthly_averages/maver.txt.

## 3. Results

Fig. 1a–b shows the height-time cross section of monthly composites of lunar tidal amplitudes in zonal and meridional winds over Tirunelveli for the years 1993–2012. The tidal amplitudes in both zonal and meridional winds show similar seasonal variations with maximum amplitudes of about 5 m/s during February/March and secondary amplitudes of about 3 m/s during September. The lunar tidal amplitudes are smaller during the summer months (May–August) in both wind components. In zonal wind, maximum amplitudes are observed at higher heights (~92 km), whereas in meridional winds, they are observed at lower heights (~88 km). Fig. 1b shows the monthly mean tidal amplitudes from Vial and Forbes (1994) model for the height region between 82 and 98 km. The model amplitudes maximize a month earlier than the observed. The observed amplitudes are relatively higher (3–5 m/s) during February–April and September–October when compared with the model values of (~1 m/s).

Fig. 2 shows the monthly variation of lunar tidal phase at 90 km over Tirunelveli. The lunar tidal phase shows a clear seasonal variation with the phase in summer leads that in winter by about 2 h. Moreover, the tidal phases in meridional wind lead that in zonal wind from January to June and September to November while the latter leads the former during July and August. Vial and Forbes (1994) model phase values at

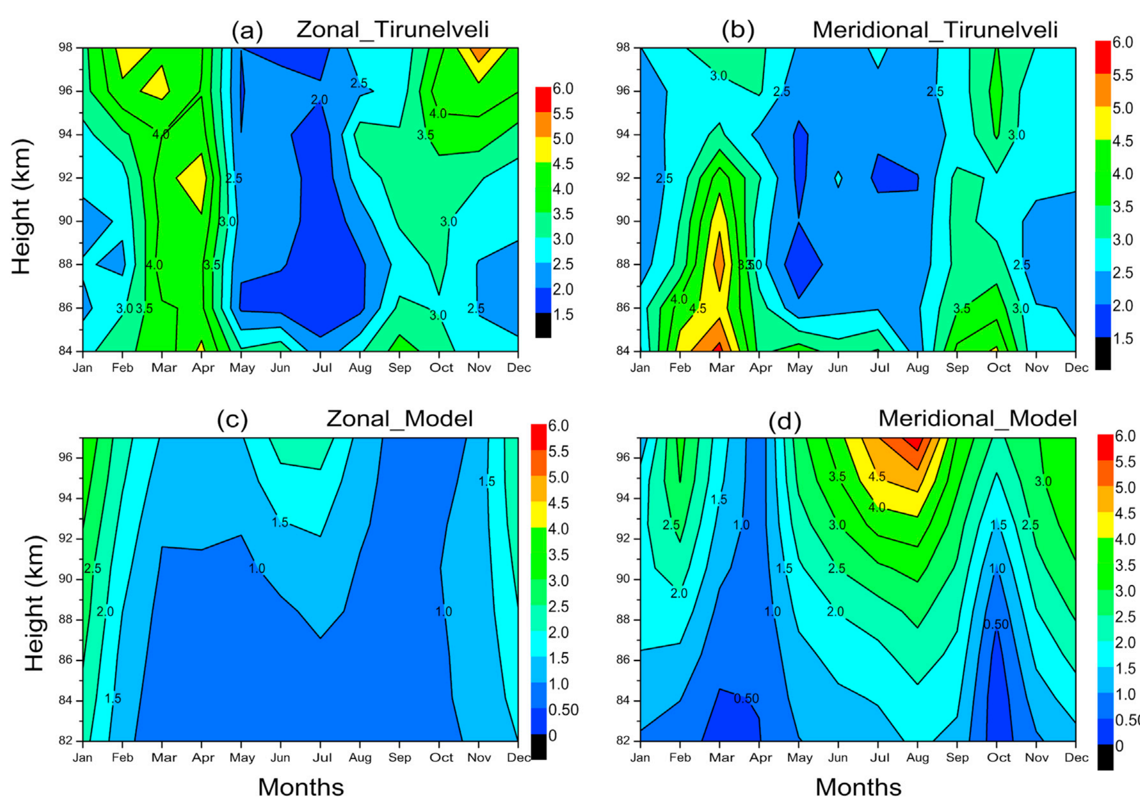


Fig. 1. Time-height cross section of lunar semidiurnal tidal amplitude of zonal (top left) and meridional wind (top right) over Tirunelveli (8.7°N, 77.8°E) for the height region 84–98 km. Bottom panel is represents the monthly mean amplitudes from Vial and Forbes (1994) model for the height region 82–97 km.

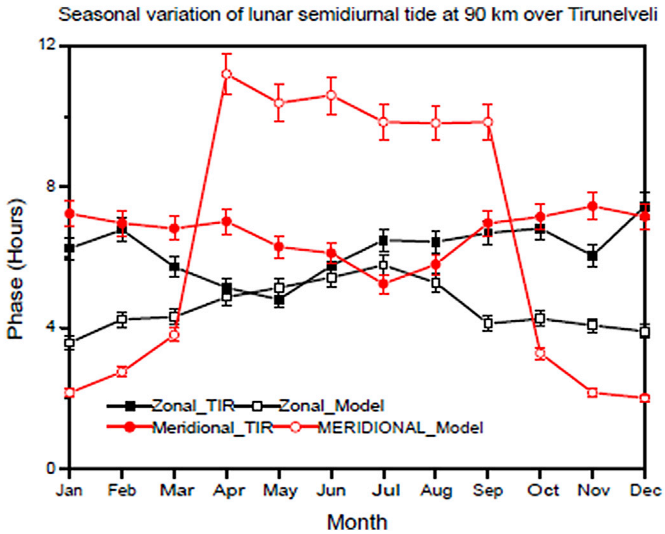


**Fig. 2.** Monthly variation of lunar semidiurnal tidal phase of zonal (filled square) and meridional (filled circle) component at 90 km along with Vial and Forbes (1994) model (unfilled) values at 90 km.

the height of 90 km are also shown in the figure for comparison. The tidal phase in zonal wind shows good agreement between observed and model values in April and June. The model and observed phase values show large discrepancies during September–December in the case of tidal phase in zonal winds and during October–December and January–March in the case of tidal phase in meridional wind. The phase values from two other equatorial latitudes (Christmas Island and Jakarta) are compared with the phase values over Tirunelveli in Table 1. The table shows good comparison of phase values over all three low-latitude sites.

Fig. 3 presents the contour plot of monthly mean amplitudes of the lunar semidiurnal tide in meridional winds for the height region 84–98 km and for the years 1993–2012. White spaces in the contours indicate data gaps. An important feature revealed is that there exists an interannual variability in the tidal amplitudes during spring equinox. The lunar semidiurnal tidal amplitude shows weaker of about ~3 m/s from 1993 to 2003 except for the years 1995 and 1999 (top and middle panels). There are also unusual amplitude enhancements during the winters of 2006 and 2009, during when major SSW occur at polar stratosphere in the northern hemisphere. Also increased amplitudes are noticed during the spring equinox months of 2004–2009.

The interannual variability of lunar semidiurnal tidal amplitude in zonal wind can be inferred from Fig. 4. The amplitudes are larger (~8 m/s) during February/March of the years 1993, 1995, 1997, 2002, 2003, 2004–2006 and 2009–2012, whereas they are weaker (~3 m/s) in the years 1994, 1996, 1998, 1999, 2001 and 2007. The tidal amplitude increases, as height increases throughout the year. Unlike observed in meridional winds, no unusual enhancement is seen during January 2006 and February 2009.

Fig. 5 shows altitude profiles of lunar semi-diurnal tidal phase in zonal (blue line) and meridional (black line) winds for each month. Corresponding theoretical phase values in zonal (green) and meridional (red) winds obtained by Vial and Forbes (1994) are also plotted for

**Table 1**
Comparison of phase values of lunar semi-diurnal tide at ~90 km over the three sites, Jakarta (JAK), Christmas Island (XMS) and Tirunelveli (TIR).

| Month | TIR | TIR | XMS | XMS | JAK | JAK |
|---|---|---|---|---|---|---|
| | Zonal | Meridional | Zonal | Meridional | Zonal | Meridional |
| January | 6 | 2 | 5 | 7 | 8 | 2 |
| June | 5 | 10 | 4 | 9 | 12 | 10 |
| March | 4 | 4 | 4 | 10 | 5 | 6 |
| September | 4.5 | 10 | 3 | 11 | 8 | 11 |

comparison. The observed phases generally decrease with height, corresponding to an upward propagating tide. Upward propagating tidal phases are observed in the meridional winds over Tirunelveli in the months of March–April (86–96 km) and September (86–90 km). However, model values show that the upward phase propagating is prominent during winter than during summer. The meridional tidal phase shows variation with height except March, April and September in all heights over Tirunelveli. The zonal phase profiles of Vial and Forbes (1994)'s model are close to the observed profiles in June–August and October–November months, whereas the meridional model values show considerable discrepancy with the observed profiles in all months. The model predicts a phase difference of 5 h between meridional and zonal winds at all heights during April–October.

In most of the months, the lunar tide shows downward phase propagation in meridional winds at heights in >92 km January and August, >88 km in February and May, >94 km in March, >90 km in April and September, >86 km in June–July and October–December. Zonal phase propagation is upwards at heights >86 km in January, >90 km in February, April–May, and November–December and >92 km in July–October. The upward phase propagation may be due to either reflection or mode coupling of tides (Paulino et al., 2015). Paulino et al. (2015) also observed increasing phases during some of the months in both components over three stations namely, São João do Cariri (7.4°S; 36.5°W), Cachoeira Paulista (22.7°S; 45°W) and Santa Maria (29.7°S; 53.7°W) over Brazilian region.

The vertical profiles of tidal phase allow the determination of the vertical wavelength of the lunar semidiurnal tide for each month. This estimation is made by least square straight line fitting the phase value with height where it shows a clear linear variation. After this, the points very far from this adjusted line have been removed and new vertical wavelength was determined. From the vertical phase variation with height, vertical wavelengths of lunar semidiurnal tide in zonal and meridional winds are computed for each month. Table 2 indicates the observed and predicted model vertical wavelengths which are calculated of zonal and meridional components. The vertical wavelength estimated from observations over Tirunelveli and the model values show that they could be different in zonal and meridional winds.

In zonal and meridional components, the vertical wavelengths of lunar tides are generally between 20 and 90 km. The vertical wavelength of lunar tide in zonal wind shows a minimum of ~28 km in March and a maximum of 76 km in the months of June and December, whereas meridional wind, the vertical wavelength shows a minimum of 17 km in May and a maximum of 62 km in the month of April. In some months, there is close agreement between the values estimated from observations and model values, in particular, during March–April in the case of lunar tide in meridional winds. There is a large discrepancy between estimated and model values in summer and fall equinox months when the model estimated vertical wavelengths can be as large as 130 km, whereas the same estimated from the observations is only in the range of 18–80 km.

The monthly mean lunar semi-diurnal tide is subjected to regression analysis as mentioned in Section 2 and the height variation of the response of these lunar tides to QBO, SC and ENSO and long-term trend in lunar tides are shown in Fig. 6 for both zonal and meridional winds. The lunar tide shows positive response in both zonal and meridional winds. The zonal tide response to QBO wind at 30 hPa is 0.012 m/s/QBO in the height region 84–90 km and the meridional tidal response to the same is 0.014–0.02 m/s/QBO in the height region 84–88 km. The zonal tide shows significant negative solar cycle response (0.4–1 m/s/100F10.7) below 90 km and positive ENSO response above 92 km, whereas the meridional tide does not show any significant response to SC and ENSO. The zonal tides shows significant increasing trend in the height region 84–94 km with a maximum of 0.067 m/s/year at 90 km, whereas the meridional tide does not show any significant trend.

## 4. Discussion and conclusions

The present long term (Twenty years, 1993–2012) observations of

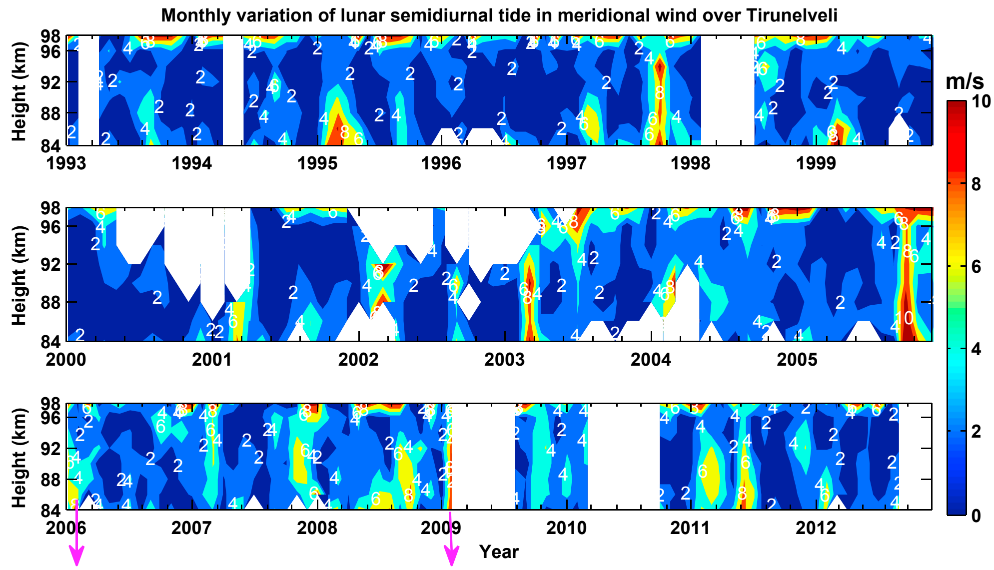


**Fig. 3.** Time-height cross section of monthly mean lunar semidiurnal tidal amplitude in meridional wind over Tirunelveli during 1993–2012.

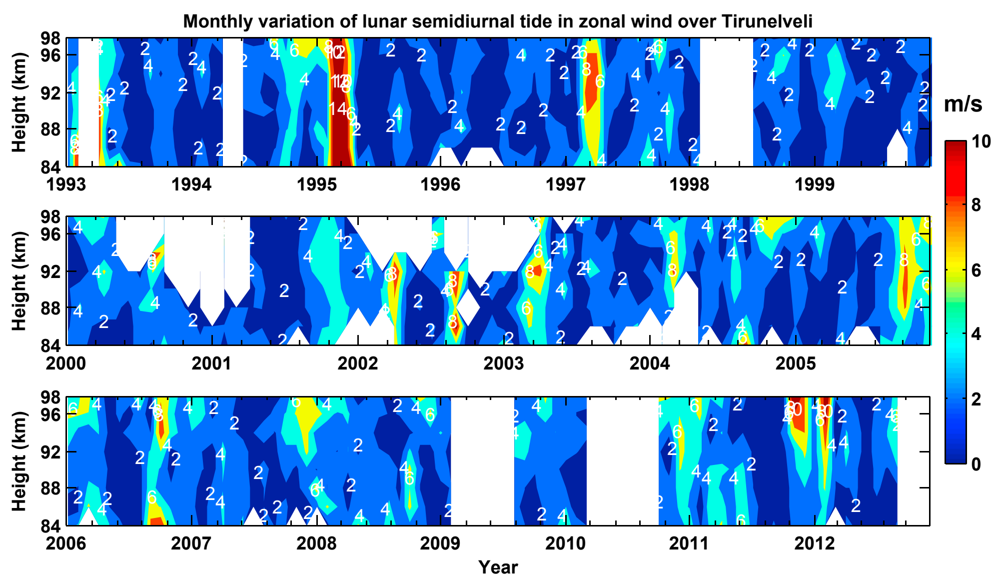


**Fig. 4.** Same as Fig. 3 but in zonal wind over Tirunelveli during 1993–2012.

mesospheric wind information obtained by the medium frequency radar at Tirunelveli (8.7°N, 77.8°E) are used to study the seasonal, interannual and long-term variabilities and tendencies of lunar semi-diurnal tide and the results are compared with model values. The tidal activities in both zonal and meridional winds show similar seasonal behavior with maximum amplitudes of about ~5 m/s during February/March, secondary maximum amplitudes of about ~3 m/s during September and minimum amplitudes during summer months (May–August). Only a few studies of the lunar semidiurnal tide in the low latitude mesospheric region have been reported. Recently, Paulino et al. (2013) reported the global view of the atmospheric lunar semidiurnal tide using Sounding of the Atmosphere Using Broadband Emission Radiometry (SABER) temperature observations and they suggested that the best conditions of propagation for the lunar semidiurnal tide are reached in the lower thermosphere region. Also, they observed an asymmetry between the hemisphere and seasonal variability is observed in the amplitude of the tide. At 90 km, they also reported peak amplitude at ±10° latitude with 90°E and 90°W during March. Our result indicates that peak amplitude is noticed during March and it is consistently observed with SABER measurements. Consistent with their reports, the present study indicates that the lunar semidiurnal tide amplitude reaches maximum during equinox and minimum during summer over Tirunelveli.

In general, the observed amplitudes in the present study compare better with Vial and Forbes (1994) model values during summer than during equinox, when the model values are larger than the observations. The variation of lunar semidiurnal tide with height at Tirunelveli does not agree with the model in some months, in particular at higher heights. In general, the model predicts much larger amplitude of the lunar tide at 90 km. The large difference between predicted and observations may be due to the presence of non-migrating lunar semidiurnal tides and longitude variations of amplitude and phase. The background wind condition plays vital role in the lunar tidal amplitude in the MLT region. (Stening et al., 2003). In different years, there are different underlying atmospheric conditions prevailing. The year to year variation of the background winds may be an indirect reason for the difference between the observed and predicted results.

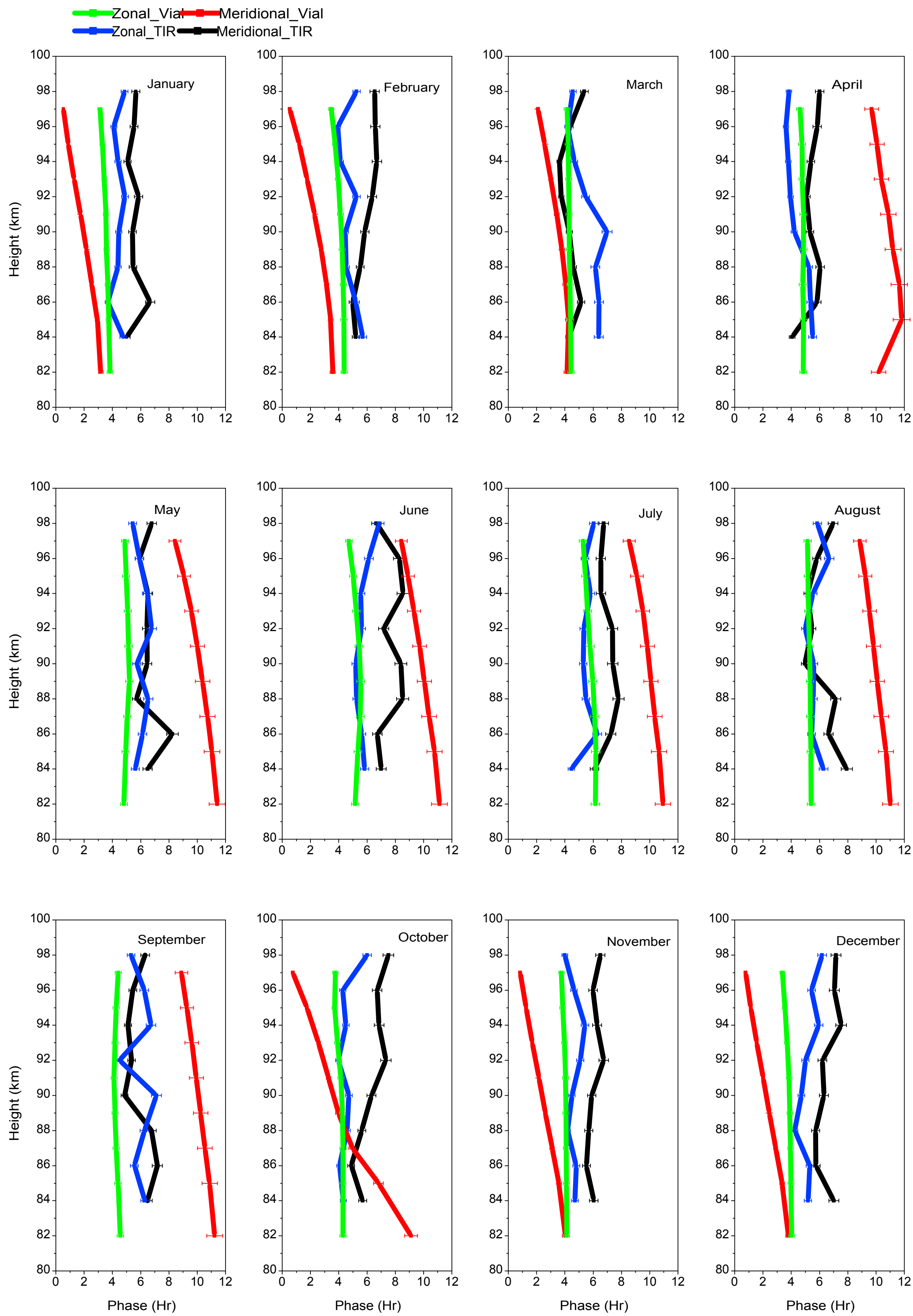


**Fig. 5.** Phases of the lunar semidiurnal tide in zonal (blue line) and meridional (black line) for each month over Tirunelveli. Vial and Forbes model phase values for meridional (red line) and zonal components (green line) are shown for comparison. (For interpretation of the references to colour in this figure legend, the reader is referred to the web version of this article.)

**Table 2**
Vertical wavelength observed at Tirunelveli (from January 1993 to December 2012) and for the model Vial and Forbes (1994). The wavelengths were calculated for both components in the height range of 84–92 km over Tirunelveli. For model, the height region of 82–97 km is used to estimate the vertical wavelengths.

| Months | TIR_U (EW) | Vial (EW) | TIR_V (NS) | Vial (NS) |
|---|---|---|---|---|
| January | | ∞ | 47 km | 98 km |
| February | 52 km | ∞ | | 57 km |
| March | 28 km | ∞ | 55 km | 75 km |
| April | 51 km | ∞ | 62 km | 46 km |
| May | | ∞ | 17 km | 62 km |
| June | 76 km | ∞ | | 68 km |
| July | 64 km | ∞ | ∞ | 78 km |
| August | 62 km | ∞ | 28 km | 87 km |
| September | | ∞ | 19 km | 78 km |
| October | | ∞ | ∞ | 24 km |
| November | 76 km | ∞ | | 57 km |
| December | 44 km | ∞ | 24 km | 59 km |

Where ∞ represents greater than 130 km.

Niu et al. (2007) studied the lunar semidiurnal tide at Wuhan (30°4N, 114.3°E) during 2002–2008 and noticed primary peak at January and secondary peak on August. They observed five lunar hours phase difference between the observed and the predicted model at 90 km in zonal and meridional components. Earlier, Stening et al. (1997) studied lunar tides in the MF radar wind measurements over Christmas Island (2°N, 157°W) in the pacific sector from 1990 to 1993 and they found that the observed lunar semidiurnal tidal amplitudes were reasonably in agree with GSWM model values with their observations. The model predicted much larger amplitudes of the lunar tide above 100 km over Collm (51°N, 13°E) (Stening and Jacobi, 2001) as observed in the present study. Recently, Lieberman et al. (2015) observed lunar semidiurnal tide globally at 250 km and 350 from CHAMP and GOCE during 2007–2008 and 2010–2011. They noticed peak during equinoctial months in both observations consistent with their WACCM-X model results.

In the present study the lunar tidal phase in meridional winds leads that in zonal winds from January to June and from September to November, while the latter leads the former during July and August. The lunar tides show large interannual variability. There are unusual amplitude enhancements in the lunar tide in meridional winds during the winters of 2006 and 2009, when SSW events occur at high latitude northern hemisphere, whereas zonal lunar tide does not show any clear association with SSW. Observations and simulations reveal that the lunar semidiurnal tide (M2) was dramatically enhanced during the 2009 SSW (Forbes and Zhang, 2012; Sathishkumar and Sridharan, 2013). The M2 enhancement is thus important to consider in simulating the ionosphere perturbations during the 2009 SSW. The vertical wavelengths of lunar tides in zonal and meridional wind are in the range 20–90 km.

The monthly mean lunar tidal amplitudes in zonal and meridional winds are subjected to regression analysis to study the tidal response to long-period oscillations, namely, QBO, SC and ENSO. It is found that the lunar tide in both zonal and meridional winds show significant positive response to QBO. Changes in the background winds in the stratosphere and mesosphere can have profound effects on the structure of the lunar tide in the upper atmosphere, while changes in the temperature variation with latitude are less important (Stening et al., 1971). Later, Lindzen and Hong (1974) and Aso et al. (1981) suggested that changes in background winds and temperature gradients could affect the propagation of the lunar tide through the atmosphere. The amplitude and height dependence of the background zonal wind have a significant influence on lunar tidal behavior (Stening et al., 2003). The zonal lunar tide over Tirunelveli shows a significant negative response to solar flux. Earlier, Huang (1979) observed a steady increase in the lunar tidal amplitude of total electron content from summer to winter and it indicates an opposite variation with solar flux. Rastogi (1968) also found similar seasonal variation of lunar semi-diurnal tide in the horizontal component of geomagnetic field over Huancayo.

To conclude the long-term MF radar wind measurements over Tirunelveli (8.7°N, 77.8°E) used to study the seasonal, interannual and long-term variabilities and tendencies of the lunar semidiurnal tide. Future study will deal with the variabilities in equatorial electrojet strength over Tirunelveli and how the mesosphere and E-region are coupled with lunar tides.

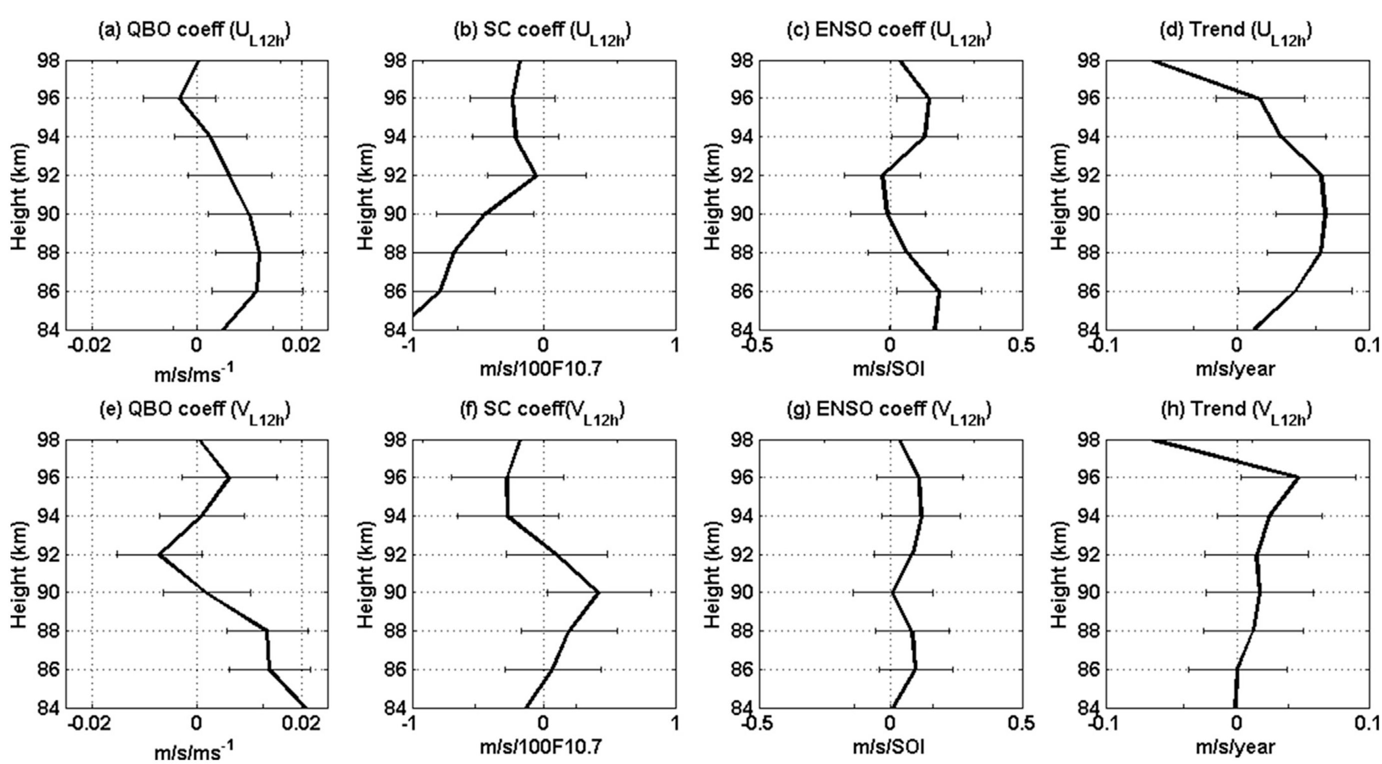


**Fig. 6.** Altitude profiles of the response of lunar semi-diurnal tidal regression coefficients (a–d) zonal winds and (e–h) meridional winds to QBO, SC and ENSO and their long-term trends.

## Acknowledgements

The QBO winds and SOI data used in the present study were downloaded from the Web at http://www.cpc.ncep.noaa.gov. The solar flux data were obtained from ftp://ftp.ngdc.noaa.gov/STP/SOLAR_DATA/SOLAR_RADIO/FLUX/MONTHLY.OBS. The Vial (1994) model values are obtained from http://cedarweb.vsp/ucar.edu/wili/index.php/Main. They thank the technical staff of Indian Institute of Geomagnetism, who maintain and successfully run the geomagnetic observatories at Tirunelveli and Alibag and the MF radar at Tirunelveli.


## References


Aso, T., Nonoyama, T., Kato, S., 1981. Numerical simulations of semidiurnal atmospheric tides. J. Geophys. Res. 86 (A13), 11388–11400. http://dx.doi.org/10.1029/JA086iA13p11388.

Burrage, M.D., Hagan, M.E., Skinner, W.R., Wu, D.L., Hays, P.B., 1995. Long-term variability in the solar diurnal tide observed by HRDI and simulated by the GSWM. Geophys. Res. Lett. 22, 2641–2644.

Chapman, S., Lindzen, R.S., 1970. Atmospheric Tides. Gordon and Breach, New York.

Fejer, B.G., Olson, M.E., Chau, J.L., Stolle, C., Lühr, H., Goncharenko, L.P., KYumoto, Nagatsuma, T., 2010. Lunar-dependent equatorial ionospheric electrodynamic effects during sudden stratospheric warmings. J. Geophys. Res. 115, A00G03. http://dx.doi.org/10.1029/2010JA015273.

Forbes, J.M., Groves, G.V., 1987. Diurnal propagating tides in the low latitude middle atmosphere. J. Atmos. Sol. Terr. Phys. 49, 153–164.

Forbes, J.M., Zhang, X., 2012. Lunar tide amplification during the 2009 stratosphere warming event: observations and theory. J. Geophys. Res. 117 http://dx.doi.org/10.1029/2012JA017963 (January, A12312).

Forbes, J.M., Zhang, X., Bruinsma, S., Oberheide, J., 2013. Lunar semidiurnal tide in the thermosphere under solar minimum conditions. J. Geophys. Res. 118, 1788–1801. http://dx.doi.org/10.1029/2012JA017962.

Huang, Y., 1979. Solar cycle and seasonal variations of the solar and lunar daily variations of total electron content at lunping. J. Geophys. Res. 84, 6595–6601.

Laskar, F., Pallamraju, D., Veenadhari, B., 2014. Vertical coupling of atmospheres: dependence on strength of sudden stratospheric warming and solar activity. Earth Planets Space 66, 94.

Lieberman, R.S., Fritts, D.C., Pedatella, N., Doornbos, E., Ortland, D.A., 2015. Global observations of thermospheric lunar tidal winds. J. Atmos. Sol. Terr. Phys. 136, 126–133.

Lindzen, R.S., Hong, S.S., 1974. Effects of mean winds and horizontal temperature gradients on solar and lunar semidiurnal tides in the atmosphere. J. Atmos. Sci. 31, 1421–1466.

Luhr, H., Siddiqui, T.A., Maus, S., 2012. Global characteristics of the lunar tidal modulations of the equatorial electrojet derived from CHAMP observations. Ann. Geophys. 30, 527–536.

Niu, X., Xiong, J., Wan, W., Ning, R., Liu, L., Vincent, R.A., Reid, L.M., 2005. Lunar tidal winds in the mesosphere over Wuhan and Adelaide. Adv. Space Res. 36, 2218–2222.

Niu, X.J., Xiong, J.G., Wan, W.X., Ning, B.Q., Liu, L.B., 2007. A measurement of the lunar semidiurnal tide at Wuhan (30°40N, 114°30E). Earth Planets Space 59, 991–997.

Pancheva, D.V., Miyoshi, Y., Mukhtarov, P., Jin, H., 2012. Global response of the ionosphere to atmospheric tides forced from below: comparison between COSMIC measurements and simulations by Atmosphere Ionosphere Coupled Model GAIA. J. Geophys. Res. 117, A07319. http://dx.doi.org/10.1029/2011JA017452.

Park, J., Lühr, H., Kunze, M., Fejer, B.G., Min, K.W., 2012. Effect of sudden stratospheric warming on lunar tidal modulation of the equatorial electrojet. J. Geophys. Res. 117, A03306. http://dx.doi.org/10.1029/2011JA017351.

Paulino, A.R., Batista, P.P., Clemeshaa, B.R., Buriti, R.A., Schuch, N., 2012. An enhancement of the lunar tide in the MLT region observed in the Brazilian sector during 2006 SSW. J. Atmos. Sol. Terr. Phys. http://dx.doi.org/10.1016/j.jastp.2011.12.015.

Paulino, A.R., Batista, P.P., Batista, I.S., 2013. Global view of the atmospheric lunar semidiurnal tide. J. Geophys. Res. 118, 13128–13139. http://dx.doi.org/10.1002/2013/JD019818.

Paulino, A.R., Batista, P.P., Lima, L.M., Clemeshaa, B.R., Buriti, R.A., Schuch, N., 2015. The lunar tides in the mesosphere and lower thermosphere over Brazilian sector. J. Atmos. Sol. Terr. Phys. 133, 129–138.

Pedatella, N.M., Forbes, J.M., 2010. Evidence for stratosphere sudden warming-ionosphere coupling due to vertically propagating tides. Geophys. Res. Lett. 37, l11104. http://dx.doi.org/10.1029/2010GL043560.

Pedatella, N.M., Liu, H.L., Richmond, A.D., Maute, A., Fang, T.W., 2012. Simulations of solar and lunar tidal variability in the mesosphere and lower thermosphere during sudden stratosphere warmings and their influence on the low-latitude ionosphere. J. Geophys. Res. 117, A08326. http://dx.doi.org/10.1029/2012JA017858.

Pedatella, N.M., Fuller-Rowell, T., Wang, H., Jin, H., Miyoshi, Y., Fujiwara, H., Shinagawa, H., Liu, H.L., Sassi, F., Schmidt, H., VMatthias, Goncharenko, L., 2014. The neutral dynamics during the 2009 sudden stratosphere warming simulated by different whole atmosphere models. J. Geophys. Res. 119, 1306–1324. http://dx.doi.org/10.1002/2013JA019421.

Randel, W.J., Cobb, J.B., 1994. Coherent variations of monthly mean column ozone and lower stratospheric temperature. J. Geophys. Res. 99 (D3), 5433–5447. http://dx.doi.org/10.1029/93JD03454.

Rastogi, R.G., 1968. Luni-solar tidal oscillations in horizontal magnetic intensity H and in foF2 at Huancayo during low solar activity. J. Atrnos. Sol. Terr. Phys. 30, 497.

Sanford, D.J., Muller, H.G., Mitchell, N.J., 2006. Observations of lunar tides in the mesosphere and lower thermosphere at Arctic and mid latitudes. Atmos. Chem Phys. 6, 4117–4127.

Sanford, D.J., Mitchell, N.J., Vincent, R.A., Murphy, D.J., 2007. The lunar tides in the Antarctic mesosphere and lower thermosphere. J. Atmos. Sol. Terr. Phys. 69, 2219–2237.

Sathishkumar, S., Sridharan, S., 2013. Lunar and solar tidal variabilities in mesospheric winds and EEJ strength over Tirunelveli (8.7°N, 77.8°E) during the 2009 major stratospheric warming. J. Geophys. Res. 118, 533–541. http://dx.doi.org/10.1029/2012JA018236.

Schlapp, D.M., Harris, T.J., 1993. Lunar tidal analysis of 6 yr of mesospheric wind data at Adelaide. J. Atmos. Sol. Terr. Phys. 55, 1629–1635.

Sridharan, S., Tsuda, T., Gurubaran, S., 2010. Long term tendencies in the mesosphere and lower thermosphere mean winds and tides as observed by medium frequency radar at Tirunelveli (8.7°N, 77.8°E). J. Geophys. Res. 115, D08109. http://dx.doi.org/10.1029/2008JD011609.

Stening, R.J., Flemming, K., Fraser, G., 1995. Upper atmosphere semidiurnal tides at Christchurch (44°S) and ScottBase (78°S). J. Atmos. Solar-Terr. Phy. 57, 857–869.

Stening, R.J., Jacobi, C., 2001. Lunar tidal winds in the upper atmosphere over Collm. Anns. Geophys. 18, 1645–1650.

Stening, R.J., Vincent, R.A., 1989. A measurement of lunar tide in the mesosphere at Adelaide, South Australia. J. Geophys. Res. 94, 10.121–10.129.

Stening, R.J., Manson, A.H., Meek, C.E., Vincent, R.A., 1994. Lunar tidal winds at Adelaide and Saskatoon at 80 to 100 km heights 1985-1990. J. Geophys. Res. 99, 13273.

Stening, R.J., Schlapp, D.M., Vincent, R.A., 1997. Lunar tides in the mesosphere over Christmas Island (2°N, 203°E). J. Geophys. Res. 102, 26,239–26,245.

Stening, R.J., Tsuda, T., Nakumara, T., 2003. Lunar tidal winds in the upper atmosphere over Jakarta. J. Geophys. Res. 108, 1192.

Truskowski, Alexander O., Forbes, Jeffrey M., Zhang, Xiaoli, Palo, Scott E., 2014. New perspectives on thermosphere tides 1. Lower thermosphere spectra and seasonal-latitudinal structures. Earth Planets Space 66, 136.

Tsuda, T., Tanii, J., Aso, T., Kato, S., 1981. Lunar tides at meteor heights. Geophys Res. Lett. 8, 191–194.

Vial, F., Forbes, J.M., 1994. Monthly simulations of the lunar semidiurnal tide. J. Atmos. Sol. Terr. Phys. 56, 1591–1607.